Nuclear Instruments and Methods in Physics Research A 849 (2017) 60–71

Contents lists available at ScienceDirect

Nuclear Instruments and Methods in Physics Research A

journal homepage: www.elsevier.com/locate/nima

Technical notes

Measurements of ^{55}Fe activity in activated steel samples with GEMPix

A. Curioni[a,b], N. Dinar[a,c], F.P. La Torre[a], J. Leidner[a,d,*], F. Murtas[a,e], S. Puddu[a], M. Silari[a]

[a] CERN, 1211 Geneva 23, Switzerland
[b] Politecnico di Milano, Piazza Leonardo da Vinci 32, 20133 Milano, Italy
[c] Université de Paris VII, 5 rue Thomas-Mann, 75013 Paris, France
[d] RWTH Aachen, Templergraben 55, 52056 Aachen, Germany
[e] INFN-LNF, Via E. Fermi 40, 00044 Frascati, Italy

ARTICLE INFO

Keywords:
Radioactive waste
X-Ray detectors
Micropattern gaseous detectors
Radiochemical analysis
Timepix
GEM

ABSTRACT

In this paper we present a novel method, based on the recently developed GEMPix detector, to measure the ^{55}Fe content in samples of metallic material activated during operation of CERN accelerators and experimental facilities. The GEMPix, a gas detector with highly pixelated read-out, has been obtained by coupling a triple Gas Electron Multiplier (GEM) to a quad Timepix ASIC. Sample preparation, measurements performed on 45 samples and data analysis are described. The calibration factor (counts per second per unit specific activity) has been obtained via measurements of the ^{55}Fe activity determined by radiochemical analysis of the same samples. Detection limit and sensitivity to the current Swiss exemption limit are calculated. Comparison with radiochemical analysis shows inconsistency for the sensitivity for only two samples, most likely due to underestimated uncertainties of the GEMPix analysis. An operative test phase of this technique is already planned at CERN.

1. Introduction

The operation of particle accelerators and experimental facilities generates activated equipment and material which, when no longer in use, become radioactive waste. This mostly weakly radioactive waste is usually stored *ad interim* at the facility premises (to allow for radioactive decay, sorting, conditioning and characterization), before it is sent to a national repository. The waste must be radiologically characterized as the repositories usually require the full radionuclide inventory before it is accepted. Radioactive waste from particle accelerators is mostly made of metallic components coming from accelerators, experimental apparatus, ancillary equipment and surrounding infrastructures. Both nuclear power plants and research laboratories, among which CERN, characterize low-level and very-low-level activity waste by exploiting the relationship between easy-to-measure (ETM) nuclides (gamma emitting nuclides whose radioactivity can be readily measured directly by non-destructive assay means), and difficult-to-measure (DTM) nuclides (radionuclides whose radioactivity is difficult to measure directly from outside of the waste package by non-destructive assay means) [1,2]. Some of them are impossible-to-measure (ITM) even in a laboratory. The scaling factor (SF) method is an approach used to evaluate these DTM and ITM nuclides [3]. A scaling factor is the mathematical relationship between the activity of a DTM or ITM and the activity of some ETM key nuclides (KN). The activities of DTM nuclides in waste packages are estimated by measuring the gamma emitting KNs through gamma-spectrometry measurements from outside the package and applying the SFs to calculate the DTM activities. The SFs can be obtained via experimental measurements (sampling, experimental scaling factors) and through analytical or Monte Carlo calculations (theoretical correlation coefficients).

At CERN, the DTM and ITM radionuclides are discriminated depending on their contribution to the Indice Radiologique d'Acceptation en Stockage (IRAS), which is a hazard factor defined by the French National Agency for Radioactive Waste Management (ANDRA) to establish criteria for waste acceptability in final repositories [4]. The radionuclides that contribute for more than 1% to the IRAS are directly measured (direct ETM measurement and Scaling Factors for DTMs) otherwise they are estimated using the Correlation Method (ITMs) [5]. The ^{55}Fe radionuclide is a DTM radionuclide present in iron and steel radioactive waste, and therefore it must be measured according to the specific characterization procedure [5].

The activity limit of ^{55}Fe for the disposal of waste as very-low-level radioactive waste ("très faiblement actif" – TFA) towards the French repository is 10 kBq/g (if ^{55}Fe is the only radionuclide present in the waste). The declaration limit, i.e. the activity limit above which ^{55}Fe

* Corresponding author at: CERN, 1211 Geneva 23, Switzerland.
E-mail address: johannes.leidner@cern.ch (J. Leidner).

http://dx.doi.org/10.1016/j.nima.2016.12.059
Received 21 October 2016; Received in revised form 20 December 2016; Accepted 29 December 2016
Available online 30 December 2016
0168-9002/

must always be declared in France is 10 Bq/g [4]. The current exemption limit of ^{55}Fe for clearance of materials according to the Swiss legislation is 30 Bq/g [6]. This exemption limit will be increased to 1 kBq/g with the introduction of the new legislation.[1]

The ^{55}Fe radionuclide is currently assessed at CERN in the TFA waste by means of radiochemical analyses on waste samples. After collection and tracking, the samples are shipped to external companies to perform the analysis. A typical delay time is about 2 months for the work performed by the company, including sample preparation (cutting and acid digestion) and liquid scintillation counting. Thanks to the separation of the chemical elements, the scintillation technique reaches a detection limit for ^{55}Fe in metals of about 0.3–0.5 Bq/g [7].

Apart from radiochemical analysis, there are a number of options to detect the characteristic 5.9 keV X-rays from ^{55}Fe.[2] For example:

1. Si detectors (Si-PIN or SDD), which provide an excellent energy resolution, between 125 and 200 eV FWHM (2–3%), typically for an active area of few tens of square millimeters.[3]
2. Scintillation detectors, e.g. NaI(Tl) with a thin entry window for the soft X-rays [8]
3. Gaseous detectors, as proportional chambers or Micropattern Gaseous Detectors (MPGD), which give a large effective area (tens of cm^2) and an energy resolution of about 20% FWHM at 5.9 keV.

In this work we have developed a measurement procedure using a novel MPGD detector called GEMPix [9].

2. The GEMPix detector

The GEMPix is a novel detector obtained by coupling two CERN technologies, a small triple Gas Electron Multiplier (GEM) detector (3×3×1.2 cm^3 active volume) to a quad Timepix ASIC with 262,144 pixels of 55×55 μm^2 area for readout (Fig. 1).

GEM detectors are a relatively recent innovation in detector technology invented at CERN by F. Sauli in 1996 [10]. The basic element is a GEM foil, which consists of a 50 μm thick insulating Kapton layer electroplated with a conductive metal on both sides. Small holes are then etched in this foil and a voltage is applied across it. This produces electrical fields as high as 100 kV cm^{-1} inside the holes. When an electron traverses the hole, avalanche multiplication takes place giving approximately 20 secondary electrons[4] for each primary electron (the exact value depends on gas density, gas mixture and applied electric field). The triple GEM configuration used in the GEMPix has gains in the range of 10^2–10^4. In the GEMPix the GEM foils are held rigid by gluing them to a frame, and the electrodes supplying the high voltage are arranged to avoid discharges onto the wire bonds of the Timepix readout. On top of the GEM/Timepix region is a 12 mm thick drift volume, topped with a Mylar cathode metallized with a thin aluminum layer (approximately 18 μm in total of which 1 μm is the aluminum layer).

A continuous flow of an Ar:CO_2:CF_4 (45:15:40 ratio) gas mixture is supplied externally at a rate of 3 l/h.[5] The whole system is made sufficiently gas tight with a thin layer of epoxy resin. An HVGEM unit [11] controls seven electrical fields (one per GEM foil, two charge transfer fields, an induction field and a drift field), shown schematically in Fig. 2. Except where otherwise noted the chamber is operated at a gain G=3×10^3 corresponding to a total applied voltage to the GEM foils of 1240 V (~450 V per foil) [12] and a drift field of 0.66 kV cm^{-1}. The quad Timepix is mounted on a bespoke quad PCB, and read out using the FITPix system [13] and accompanying Pixelman [14] software.

The Timepix [16] is a pixelated silicon detector developed by the Medipix Collaboration [17,18]. It is based on a read-out chip consisting of a 256×256 pixel CMOS ASIC to which different pixelated semiconductor sensors are normally bump-bonded. It has seen wide applications in particle tracking [19,20], as an educational tool [21,22] and in dosimetry [23,24]; it is currently commercially available from various companies. In this application, however, we use a 2×2 array of chips (for a total of 512×512 pixels) without silicon sensor as readout for a triple GEM detector. Each pixel measures 55×55 μm^2. The salient feature of the Timepix is that the processing electronics for each pixel, including a preamplifier, discriminator threshold (set at a minimum value of about 1000 electrons for noise free operation) and 13.5 bit pseudo-random counter (counts up to 11,818) fit inside the footprint of the overlying semiconductor pixel. The Timepix contains a global clock which is operated at 48 MHz.

One of three modes can be used for each pixel: Counting (Medipix), Time Of Arrival (TOA) and Time Over Threshold (TOT). The mode that has been used for this measurement is the TOT mode. In this mode whenever the pulse is above threshold the pixel counts until the pulse is low again. This allows each pixel to act as a Wilkinson type ADC measuring the discharge time of the preamplifier (i.e. the time spent over the threshold). Fig. 3 shows schematically how the TOA and TOT modes of operation work. The Timepix operates with a frame based readout. This means that the chip possesses a digital shutter, and the pixels only count when the shutter is open. After the shutter closes the Timepix is then read out before acquiring a new frame.

The FITPix system and the accompanying Pixelman software are used to readout the GEMPix. The Pixelman can be run using Python scripts that define the main parameters (thresholds, polarity, trigger type, etc.), initialize the detector and perform the frame readout, typically with a time gate of 1 s. There is also the possibility to use an algorithm inside the Python script to perform an online cluster analysis for a better analysis of the particle interacting in the drift volume. Fig. 4 shows a frame picture taken with 1 s time gate, in which the clusters produced by 5.9 keV X-rays coming from ^{55}Fe and the tracks produced by Compton electrons or cosmic rays can be easily distinguished.

3. Experimental technique

^{55}Fe is a radioactive isotope of iron decaying by electron capture to ^{55}Mn with a half-life of 2.7 years. The electron capture is followed by emission of the characteristic 5.9 keV X-rays. Due to their low-energy, the photons are strongly absorbed within a few μm of the material. On the other hand, radionuclides such as ^{60}Co, ^{54}Mn, ^{44}Ti emitting photons of higher energies and therefore longer attenuation lengths, are usually present together with ^{55}Fe in activated metallic waste. A direct measurement of the X-rays of ^{55}Fe thus requires a drastic reduction of the sample thickness in order to decrease the gamma background. For this purpose, the samples need to be ground and a thin layer of metallic powder shall be used for the measurements with the GEMPix.

This can be shown by calculating the self-attenuation of a sample when measuring the ^{55}Fe X-rays with an underlying background of ^{60}Co photons. Two simplifying assumptions are made: first, the problem is one-dimensional such that geometrical effects are neglected. Second, ^{55}Fe is equally distributed in the sample such that the emission probability is position-independent in the sample. The same assumption holds for ^{60}Co. The ratio of number of photons escaping from the sample over number of photons

[1] New limits to be introduced in the process of the general revision of the Swiss regulations concerning radiation protection: http://www.bag.admin.ch/themen/strahlung/02883/03200/index.html?lang=fr.

[2] A concise review of detectors for X-rays can be found in the X-Ray Data Booklet, Sec. 4.5, available on-line http://xdb.lbl.gov/Section4/Sec_4-5.pdf

[3] As an example of off-the-shelf X-ray detectors: http://amptek.com/x-ray-detector-selection-guide/.

[4] This number is the effective multiplication per GEM foil, taking into account that some electrons are captured by the lower side of the GEM foil. The triple GEM configuration with a rather low gain per foil was chosen in order to achieve a reliable system without discharges.

[5] Other, cheaper gas mixtures such as Ar:CO_2 could be used instead. However, the fast drift velocity of Ar:CO_2:CF_4 is needed in other applications of the GEMPix to reduce the lateral electron diffusion and therefore to increase the cluster analysis performance [15].

Fig. 1. The GEMPix detector: (1) external gas supply, (2) external HV connector, (3) Mylar window, (4) frame to hold the GEM foils, (5) FITPix readout.

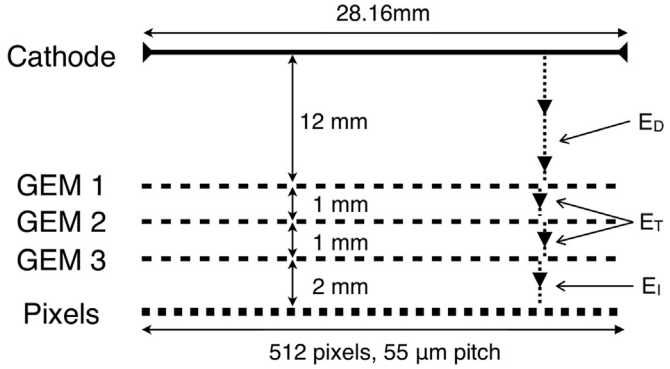

Fig. 2. The schematic of the detector including the principle dimensions and transport fields (ED=drift field, ET=transfer fields, EI=induction field) [15].

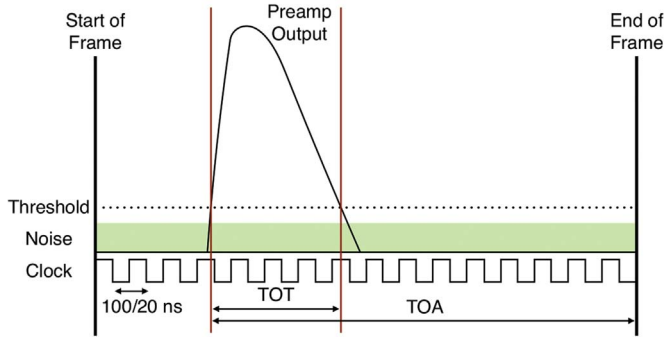

Fig. 3. The TOT mode in the Timepix ASIC measures the time elapsed while the preamp output is high against the threshold discriminator. The TOA mode measures the time from when the preamp goes high against the threshold until the end of the acquisition frame [15].

emitted in the sample is then described by:

$$\frac{N_{photons,\ escaped}}{N_{photons,\ emitted}} = \int_0^t \frac{1}{t}\exp\left(-\frac{x}{\lambda}\right)dx = \frac{\lambda}{t}\left[1-\exp\left(-\frac{t}{\lambda}\right)\right] \quad (1)$$

where t is the thickness of the sample, x is the depth inside the sample and λ is the attenuation length of the x-rays or γ-rays photons in the sample material.

For an iron sample with a thickness of 1 cm, only 0.15% of the ^{55}Fe X-rays but 81% of the ^{60}Co photons escape from the sample.[6] However

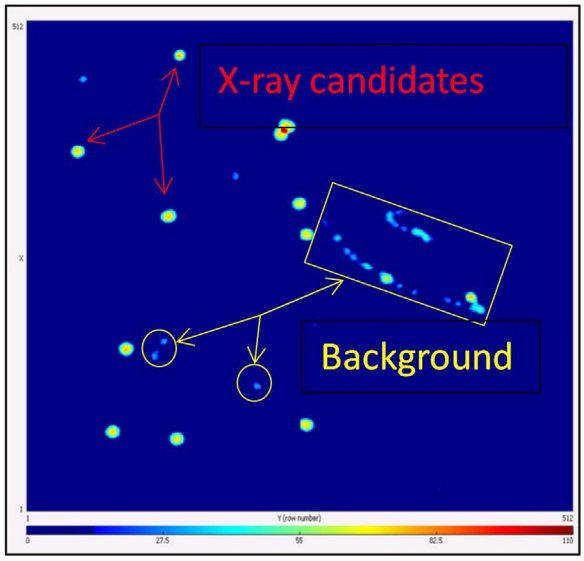

Fig. 4. The online event display of a frame acquired with a time gate of 1 s.

if the sample thickness is reduced to 100 µm, 15% of the x-rays and almost 100% of the ^{60}Co photons escape from the sample. Therefore, the signal-to-background ratio increases approximately by a factor of 80 (from 0.0019 to 0.15, assuming equal activity for ^{55}Fe and ^{60}Co and modeling the detector as a fully efficient counter without any energy resolution). Fig. 5 shows the fraction calculated by Eq. (1) for 6 keV photons for different sample thicknesses.

The operational procedure is the following. A piece of metal from the waste to be examined is selected and cut. This sample is put in a milling machine to produce about 1 g of powder and for this purpose two different tools have been used, a DEKEL FP4M and a modified Astoba. The typical parameters used for the powder production are: rotation velocity of the pin: 400 rot/min, advance velocity: 400 mm/min, cutter: MTC TiAlN 6 mm Garant (ref SFS 205712 6°). Another method is presently under investigation using a drill with a conical file to produce the powder.

The sample powder is filtered with a 0.5 mm mesh and placed in a plastic container with dimension 4×4×1 cm^3, attached to its bottom with a double-sided tape, and then gently beaten with a tool (parallel punch) to improve the adhesion of the powder to the bottom of the container. The extra powder is finally removed. The final thickness of the sample is around 100 µm.[7] Fig. 6 shows the filled sample container.

The experimental setup is schematically shown in Fig. 7. The

[6] Attenuation lengths in iron are 15 µm for 6 keV photons and 2.34 cm for 1.25 MeV photons. These values are calculated using mass attenuation coefficients and the density of iron in NIST data [25]. Tabulated values are available only for certain energies, therefore values for 6 keV and 1.25 MeV are used for ^{55}Fe (5.9 keV X-Rays) and ^{60}Co (1.17 and 1.33 MeV photons) respectively.

[7] This is an approximate average value. The average value has to be smaller than the mesh size but it is difficult to determine due to fluctuations in the grain size and grain shape.

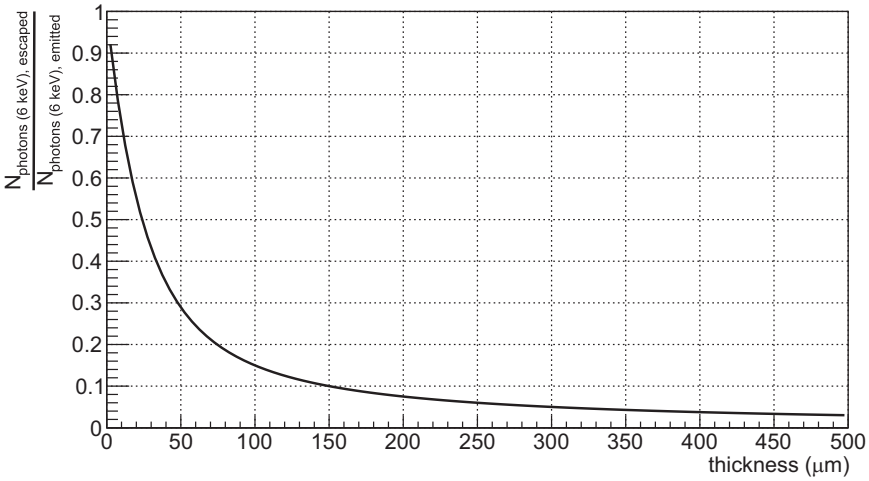

Fig. 5. Fraction of escaped over emitted 6 keV photons versus sample thickness. The corresponding fraction for 1.25 MeV photons (^{60}Co background) is larger than 98% for the shown thickness range. The plotted value is thus approximately equal to the expected signal-to-background ratio.

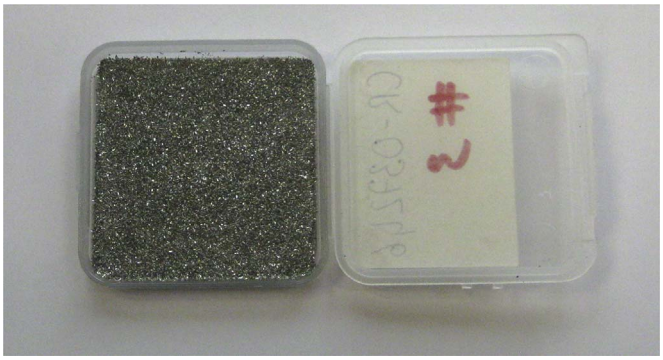

Fig. 6. The plastic container with the sample powder attached on the bottom.

detection gas (Ar:CO_2:CF_4, 45:15:40) is supplied by a 50 l bottle equipped with a gas adaptor to reduce the pressure from about 150 bar to about 1 bar. A flowmeter controls the gas flow which is set at 3 l/h. High Voltage (1240 V) is supplied by a NIM Module HVGEM and controlled by a Labview programme. A low voltage supply for the GEMPix (3.3 V) is also necessary. The GEMPix data are acquired by the FITPix module [13] and read out by the Pixelman software (Fig. 8), which includes a Python plugin for code development [14]. The GEMPix detector is placed in a lead shielding box to reduce the background produced by ambient gamma rays.

The actual search of the ^{55}Fe content in a metallic sample consists of four separate measurements: 1) calibration of the system using a source of ^{55}Fe to define the energy window for counting (next section); 2) X-ray counting of the sample; 3) calibration measurement to define the energy window for counting for the background measurement; 4) measurement of the gamma background from the sample. This is obtained by placing a thin layer of aluminum (approximately 100 μm thick corresponding to 3 attenuation lengths for 6 keV photons[8]) between sample and detector to absorb the 5.9 keV photons. Standard acquisition parameters set in Pixelman are: one second per frame, threshold of 36 counts,[9] software trigger (500 events), ToT mode, internal clock set at 48 MHz and 7200 frames (2 h) for the sample and background measurements. The calibration measurements for sample and background both last 10 min.

4. Data analysis

4.1. Online analysis

A window in the acquisition software displays the main statistics of the X-ray spectra and the time evolution of the measurements. The output of the cluster analysis is saved in a file event by event. Nineteen parameters are saved including event time, number of clusters per event, cluster type, cluster size, cluster position and total charge. Two cuts are applied in the analysis (online and offline) using some of these parameters: only clusters 'heavy blobs' are used and clusters at the edges of the chips are discarded. Heavy blobs are the typical clusters produced in the GEMPix by low energy X-rays. They fulfill the following criteria[10] [26]:

- Minimum inner pixel count: 4
- Minimum ratio of inner and border pixels: 0.5
- Maximum deviation from perfect circle[11]: 1.2

Clusters at the edges of the readout chips are discarded since they might not be fully contained in the chip and therefore their measured parameters can be incorrect. Also, edge effects of the quad Timepix ASIC exist which require an increased discard region at the edges. Therefore clusters must fulfill the following position conditions:

- 25 < centx < 246 or 266 < centx < 487
- 25 < centy < 246 or 266 < centy < 487

where centx (centy) is the x (y) coordinate of the centre of the cluster position in pixel count.

4.2. Offline analysis

Fig. 9 shows the energy spectrum of a measurement with a ^{55}Fe source. An energy resolution of about 20% FWHM is typically achieved. A Gaussian function is fit to the data obtained from the calibration measurement with a source. Mean and sigma of this fit define the counting interval for the analysis of the sample and background measurements: only events within the range "mean ± 2 sigma" are taken into account. Fig. 10 shows the energy spectrum of a sample measurement.

[8] Attenuation length in aluminum is 32 μm for 6 keV photons. This value is calculated using the mass attenuation coefficient and the density of aluminum in NIST data [25].

[9] This is equal to an energy threshold on the order of 100 eV.

[10] Using default settings in Pixelman.

[11] Defined as ratio of diameter calculated from cluster size and maximum distance within the cluster.

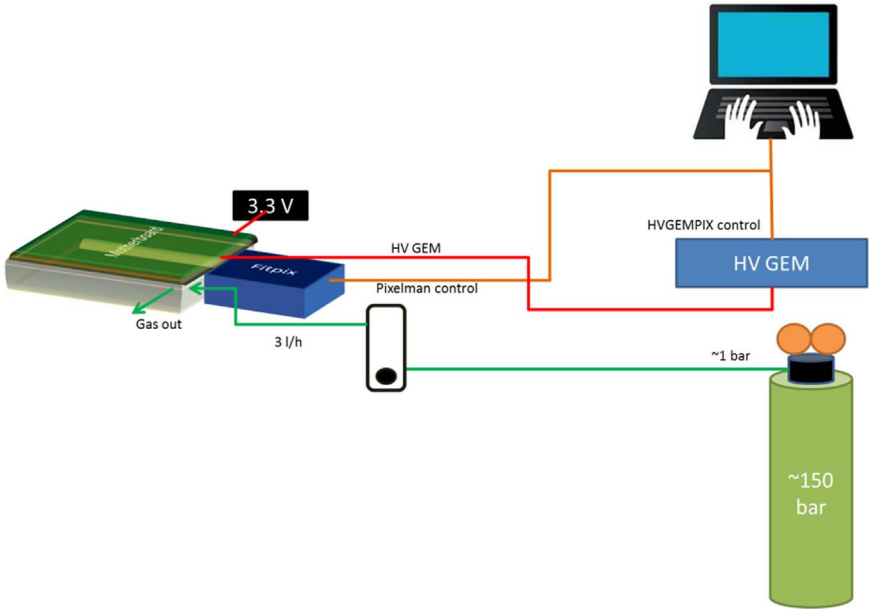

Fig. 7. Measurement setup.

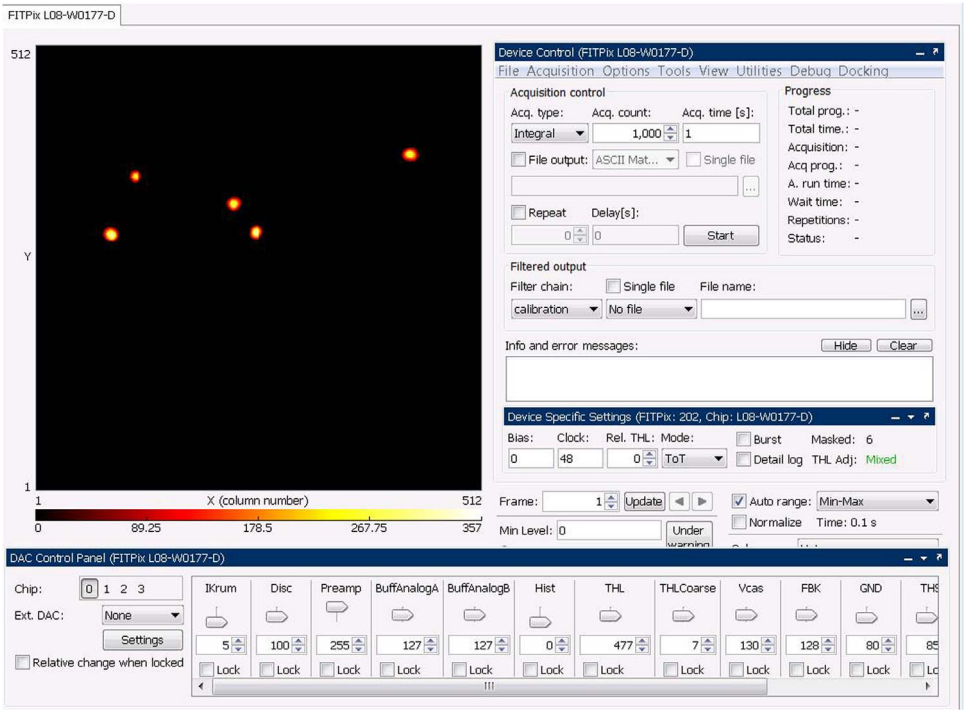

Fig. 8. The Pixelman console [14] showing the ^{55}Fe X-rays observed online during the acquisition.

5. Samples, radiochemical analysis and GEMPix results

A total of 45 activated steel samples were selected to characterize the technique. Each sample was divided in two pieces: one was sent to an external company for radiochemical analysis (AMEC [27]), the other was reduced to powder as described above and measured with the GEMPix.

A correction was applied to the radiochemical results in order to take into account the radioactive decay of ^{55}Fe due to the time difference between the GEMPix measurements and the radiochemical analysis. Most of the GEMPix measurements lasted 7200 s (2 h), the others were normalized to this duration. The shortest measurement lasted 5700 s. The background was measured as described above for 16 samples with high expected background. For the other samples, an estimated background of 50 counts in 7200 s is used instead. This is based on the fact that the lowest measured background in 7200 s is 42 counts, which implies that the true mean value of the lowest background is somewhat larger. Furthermore, the estimation of 50 counts leads to an offset in the fit of the calibration curve (Fig. 11) that is compatible with zero. For the GEMPix analysis, only statistical uncertainties on the number of counts are taken into account.

The GEMPix net counts per second (cps) are plotted against the corresponding radiochemical results in Fig. 11. An error-weighted linear fit is used to provide the conversion factor between GEMPix cps and the declared specific activity from the radiochemical analysis (Bq/g). The slope of the fit provides the calibration factor for the GEMPix:

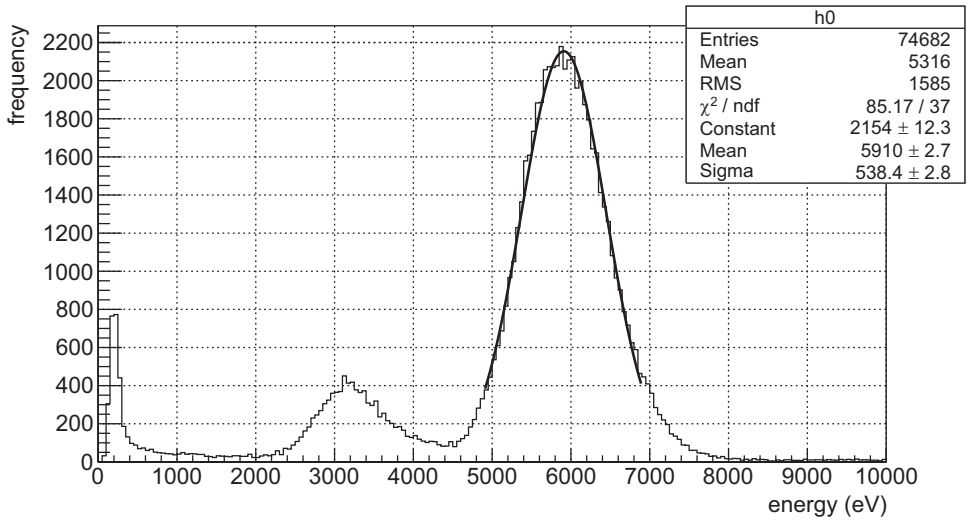

Fig. 9. Energy spectrum recorded with a ^{55}Fe calibration source. Peaks are due to ^{55}Fe x-rays (5.9 keV) and Argon escape/fluorescence (2.9 keV/3.0 keV). Here, events within (5910 ± 1077) eV would be counted in the sample and background measurements.

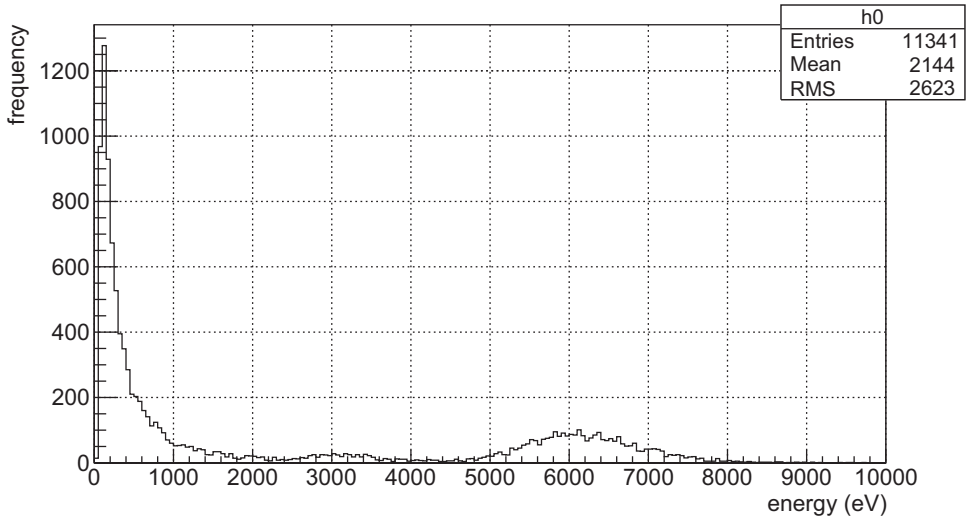

Fig. 10. Energy spectrum of a sample measurement. Only events within the energy window defined by the source measurement are counted.

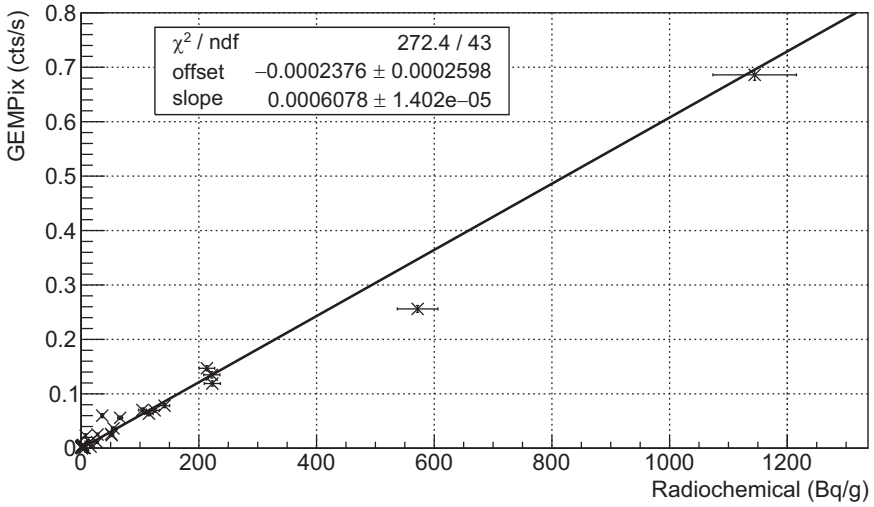

Fig. 11. GEMPix counts per second versus specific activity as determined by the radiochemical analysis. The slope of the linear fit provides the conversion factor: 1645 ± 38 (Bq/g)/(cps).

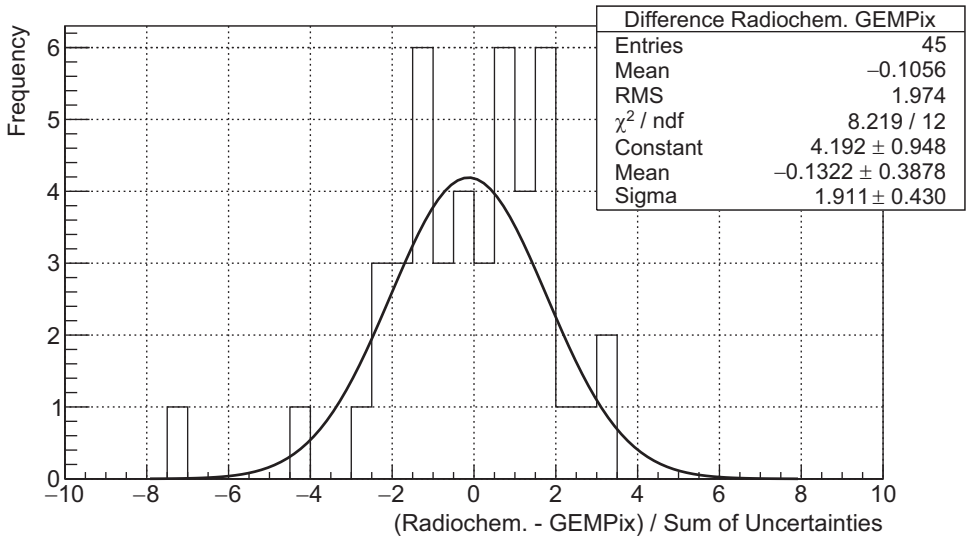

Fig. 12. Comparison between results of radiochemical analysis and GEMPix analysis in units of their uncertainties and a Gaussian fit to the distribution.

$$\left[(6.\,078 \pm 0.\,140) \times 10^{-4}\,\frac{cps}{Bq/g}\right]^{-1} = 1645 \pm 38 \quad \frac{Bq/g}{cps}.$$

The bad quality of the fit (χ^2/ndf=272/43) is explained by an underestimation of the uncertainties on the GEMPix counts, since only statistical uncertainties are considered.

Fig. 12 shows the distribution of the difference in units of the sum of the uncertainties of the two methods. The uncertainties of the two methods are added linearly to obtain the uncertainty on the difference. A Gaussian distribution is expected. The obtained distribution is well fitted by a Gaussian, but the sigma of the fit is larger than 1 and there are some outliers up to 7 sigmas. This indicates most probably an underestimation of the uncertainty, due to the fact that uncertainties on the GEMPix results are small compared to those of the radiochemical analysis since only statistical uncertainties are taken into account.

6. Sensitivity of the technique, detection limit, confidence levels and uncertainties

In this section, a Confidence Level (C.L.) of 95% is chosen for all calculations. As an example, the sensitivity to a 30 Bq/g limit is calculated as this value is the current Swiss exemption limit for ^{55}Fe. The measured background is not independent of the sample itself since there is a non-negligible contribution from other radionuclides present in the sample. Fig. 13 shows the distribution of the background measured for 16 out of 45 samples.

Detection limits of the technique are calculated depending on the background using Poisson statistical methods. The 95%-C.L. single-sided upper limits for each number of background counts is calculated according to [28]: for count numbers, n, smaller than 51 the upper limit is taken directly from a table provided in [28], for larger count numbers the upper limit, u.l., is approximated by a formula given in [28] [12]:

$$u.\,l. = (n+1)\left(1-\frac{1}{9(n+1)}+\frac{1.\,65}{3\sqrt{n+1}}\right)^3 \tag{2}$$

Fig. 14 shows the resulting upper limits for each number of background counts. These upper limits are interpreted as the detection limit above which ^{55}Fe content is detected. For example, if 100 background counts and 110 (150) total counts are measured, the result is (is not) compatible with the background-only hypothesis at 95% C.L. Fig. 15 shows the detection limit as an activity for each number of background counts. The detection limit is well below 10 Bq/g for all background counts of the 45 samples. Note that this is only the statistical detection limit. This detection limit is not reached in practice due to larger systematic uncertainties.

Fig. 16 compares the GEMPix results with the calculated detection limit. Also, the total number of counts for a sample with an activity of 30 Bq/g is calculated for each number of background counts. For this, the activity of 30 Bq/g is converted to number of counts using the calibration factor and the number of background counts is added. The 95% C.L. single-sided lower limit for the exemption limit plus background is calculated using the tables provided in [28], Eq. (2) for the upper limit for more than 50 counts, and the following Eq. (3)[13] for the lower limit, l.l., in case of more than 50 counts, n.

$$l.\,l. = n\left(1-\frac{1}{9n}-\frac{1.\,65}{3\sqrt{n}}\right)^3 \tag{3}$$

Thus, if a data point is:

- Below detection limit, the total number of counts is compatible with the background only hypothesis.
- Above detection limit, the background only hypothesis is ruled out and we infer that there is some ^{55}Fe content in the sample.
- Below the lower limit of the exemption limit, the activity of the sample is less than 30 Bq/g.
- Above the lower limit of the exemption limit, we cannot exclude an activity larger than 30 Bq/g.

All statements are at 95%-C.L.

Furthermore, Fig. 16 shows a comparison with radiochemical analysis with different marker styles and colors. If a data point is a:

- Red upwards pointing triangle: the activity of the sample measured by radiochemical analysis is larger than 30 Bq/g minus its uncertainty at 95% C.L.
- Green downwards pointing triangle, the activity of the sample measured by radiochemical analysis is smaller than 30 Bq/g minus its uncertainty at 95% C.L.

Results of the radiochemical analysis and of GEMPix are inconsistent

[12] Eq. (9) in Ref. [28].

[13] Eq. (12) in the reference.

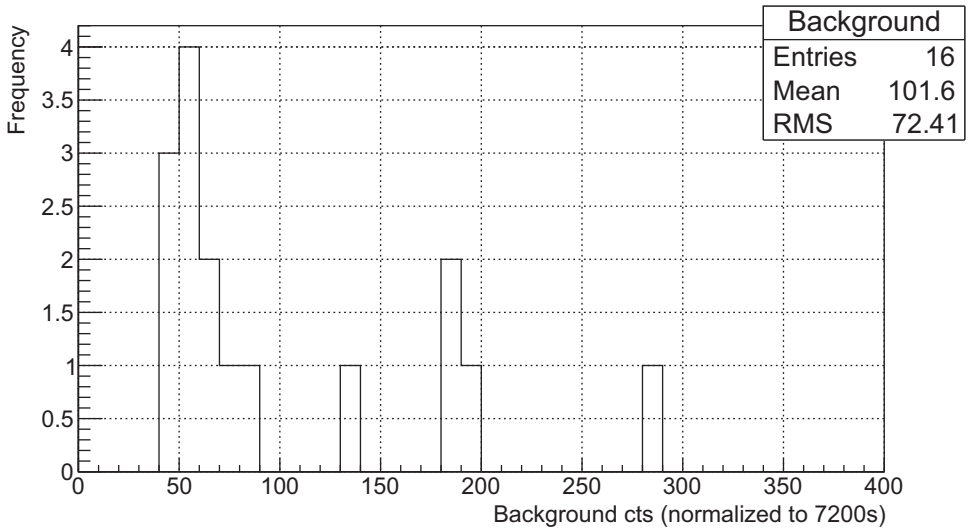

Fig. 13. Distribution of the background measured for 16 samples.

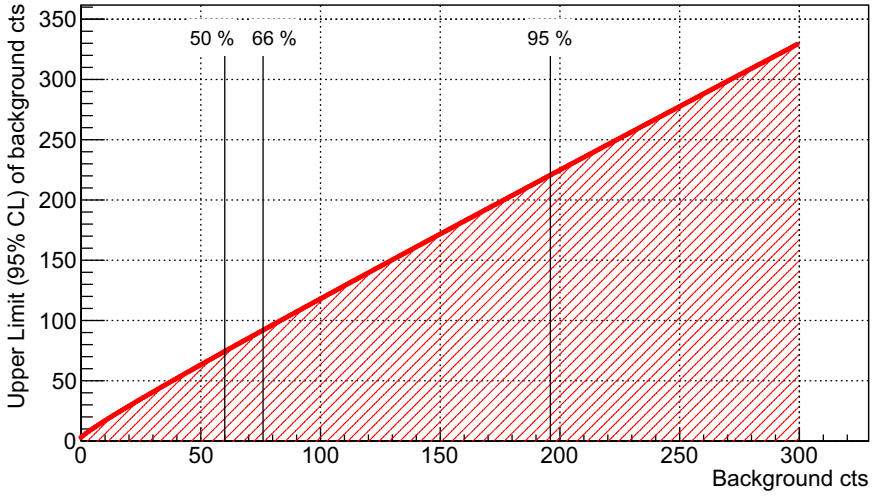

Fig. 14. The upper limits are calculated for each number of background counts (red points). Above this limit, the detector is sensitive to ^{55}Fe. Below this limit, in the shaded area, background only cannot be excluded. The vertical lines show the maximum background counts for a stated fraction of the measured samples (numbers above the lines). (For interpretation of the references to color in this figure legend, the reader is referred to the web version of this article.)

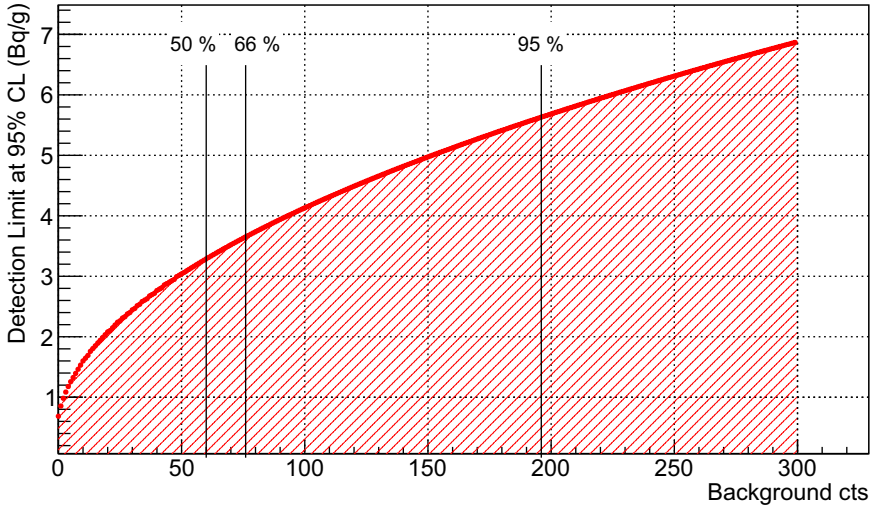

Fig. 15. The upper limits shown in Fig. 14 are background subtracted and then converted to activity using the calibration factor. Above the limit, the detector is sensitive to ^{55}Fe. Below this, in the shaded area, background only cannot be excluded. The vertical lines show the maximum background counts for a stated fraction of the measured samples (numbers above the lines). (For interpretation of the references to color in this figure legend, the reader is referred to the web version of this article.)

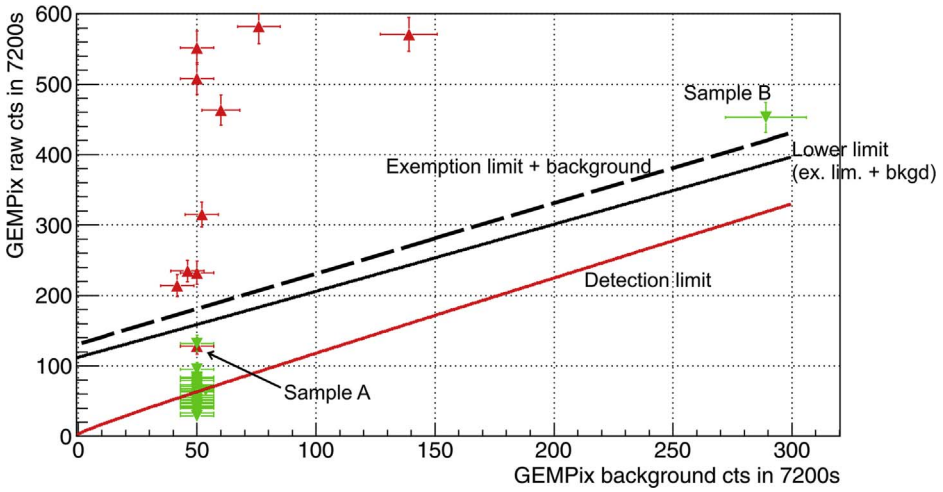

Fig. 16. GEMPix raw versus background counts (data points) of the samples are compared with the detection limit (solid red line, compare Fig. 14) and the Swiss exemption limit of 30 Bq/g plus background (black dashed line). Solid black line shows 95%-C.L. lower limit of the exemption limit plus background. Radiochemical analysis results are encoded for sample data points: red upwards (green downwards) pointing triangles denote activity plus uncertainty at 95%-C.L. above (below) exemption limit. Some samples are out of range on the y-axis of this plot but they are well above the detection limit and all are correctly assigned to have an activity larger than 30 Bq/g. (For interpretation of the references to color in this figure legend, the reader is referred to the web version of this article.)

for two of the 45 samples: for sample B the GEMPix states an activity above 30 Bq/g while the radiochemical analysis states an activity below 30 Bq/g. The results for sample A show the inverted situation. Thus, sample A would be falsely declared to have an activity below the exemption limit. However, it is expected that a complete uncertainty investigation of the GEMPix would result in larger uncertainties. The probability to falsely state that an activity is below 30 Bq/g would be decreased. At the same time, a larger uncertainty on the GEMPix results will correspondingly reduce the sensitivity. This is less problematic for larger exemption limits since the majority of ^{55}Fe samples typically has a rather low activity. The future Swiss exemption limit will be 1000 Bq/g.

The complete analysis presented in this section is limited by the fact that only statistical uncertainties on the counting are considered. An investigation of other uncertainties is necessary before defining operational limits with respect to the Swiss exemption limit. Sources of other uncertainties include sample preparation, stability of the GEMPix and positioning of the samples below the GEMPix.

7. Improvement on gain stability and HV correction of the GEMPix

A procedure for a more stable operation of the detector has been implemented: ambient conditions – pressure, temperature and humidity – are monitored and the detector HV is corrected to obtain a stable gain. This procedure increases the gain stability of the detector.

A sensor to measure pressure, temperature and humidity has been installed inside the detector. Fig. 17 shows this sensor mounted on the GEMPix readout board. Data recorded by the sensor are used to correct the High Voltage of the GEMPix and thus ensure a more stable GEM gain. First, data are acquired without any HV correction using a ^{55}Fe source. An exponential dependence of the peak position on temperature/pressure (T/P) is expected, as described for example in [29]. Fig. 18 shows measured peak positions for different T/P values and an exponential fit to the data.

To calculate a correction formula for the detector HV, it is necessary to know the dependence of the ^{55}Fe peak position on the HV. This is measured by performing a gain scan. Fig. 19 shows the results and an exponential fit that describes this dependence. In an attempt to cover a large range of the possible gain values also for other applications, not only a ^{55}Fe source but also a ^{241}Am source was used. The determination of the energy deposition and thus TOT counts is more difficult for ^{241}Am (α-source) than for ^{55}Fe (X-ray source). Also, the measurement

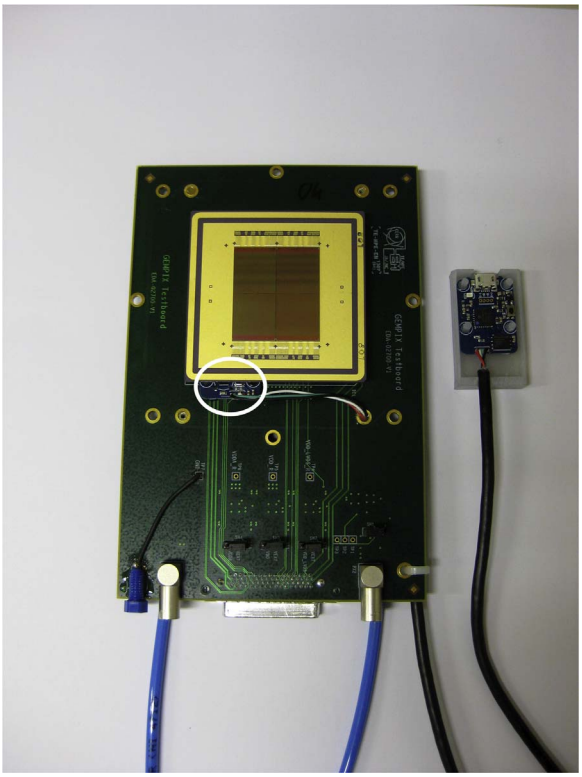

Fig. 17. Sensor for pressure, temperature and humidity (white circle) installed on the GEMPix readout board. The sensor is read out via USB.

for the lowest gain for the ^{55}Fe-source (at 1135 V) is difficult since the ^{55}Fe peak is almost in the noise. This results in a very poor fit quality. However, the model fits better in the region of interest for this technique (at 1240 V) and only the slope is used, as explained below.

A correction formula for the applied voltage, V, is derived by using the following two equations:

$$TOT'(T/P) = 5.\,9\text{keV}*\frac{TOT}{p0*\exp\,(p1*T/P)} \tag{4}$$

$$TOT'(V) = A*\exp(B*V) \tag{5}$$

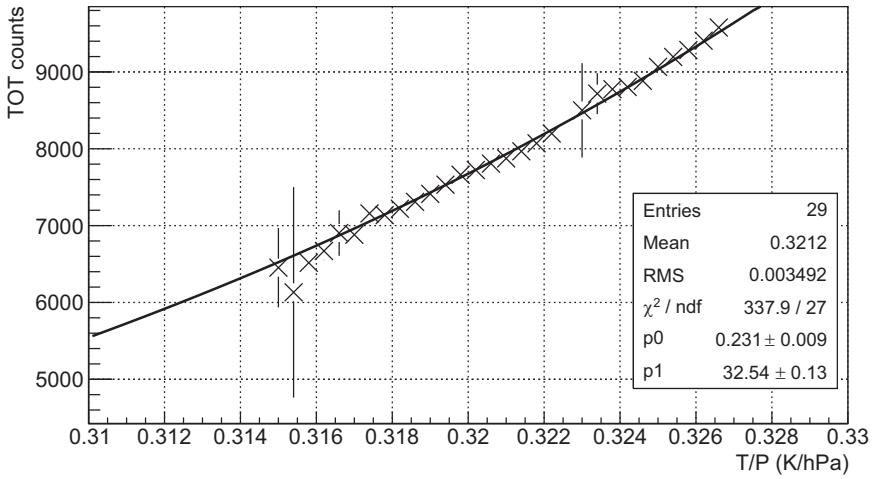

Fig. 18. The TOT counts show an exponential dependence on T/P.

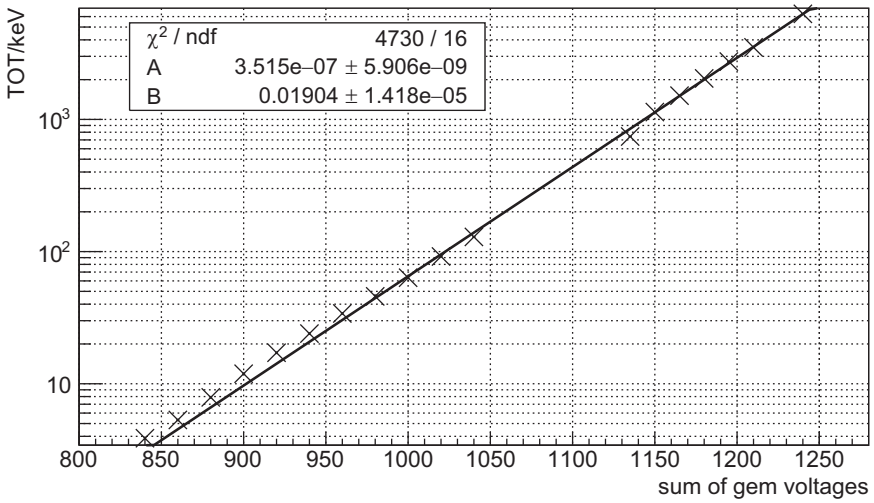

Fig. 19. Results of the gain scan with ^{55}Fe (data taken with sum of gem voltages larger than 1100 V) and ^{241}Am sources (data taken with sum of gem voltages smaller than 1100 V).

Eqs. (4) and (5) are set equal, since $TOT'(T/P) = TOT'(V)$. The comparison of the two equations thus yields:

$$V = \frac{1}{B} * \ln\left(\frac{5.9 \quad keV * TOT}{A * p0}\right) - \frac{p1}{B} * \frac{T}{P} = V_{set} + C - \frac{p1}{B} * \frac{T}{P} \tag{6}$$

Constants p0, p1, A, B can be found as fit results in Figs. 18 and 19, respectively. The first, constant part of Eq. (6) can be split up into the set voltage, V_{set}, and a new constant C. The calculated result for constant C is not used. Instead, the constant is determined experimentally such that the ^{55}Fe peak yields on average 6000 TOT counts.[14] Since systematic deviations in the gain stability are observed with this correction, a second-order correction is introduced using the humidity measurement, H. Data are acquired with the T/P-correction of Eq. (6). The analysis is done similarly to the calculation of the T/P-correction. The final correction formula to calculate the voltage is:

$$V(T/P, H) = V_{set} + 538V - 1709.03\frac{\text{V hPa}}{\text{K}} * \frac{T}{P} + 2.59\frac{V\text{m}^3}{\text{g}} * H \tag{7}$$

Measurements have been performed over nine days using this correction (Fig. 20). If the detector is flushed with gas and the HV is on continuously, a gain stability within (6000 ± 200) TOT counts is achieved. Fig. 21 demonstrates the conversion of this deviation of the mean TOT counts into an uncertainty on the number of event counts. The mean value of a Gaussian TOT count distribution with a constant resolution (sigma/mean=constant) and a constant total integral is varied. The integral for a fixed range from 4800 to 7200 TOT counts is presented in dependence of the mean TOT value. The calibrated activity depends linearly on the number of counts. Therefore, relative uncertainties on the number of counts and the activity are the same. As shown in Fig. 21, a mean TOT value of 5800 (6200) instead of 6000 transforms into a deviation of the number of events and thus on the activity of −1.1%(−0.4%). Thus, activity measurements are stable within approximately 1% with the applied HV correction. It is however not recommended to perform measurements over a longer period without control measurements with a source. This is a rather quick, independent check of the whole measurement system. Large effects will be noticed immediately, and small changes can be corrected by adjusting constant C in Eq. (6).

8. Conclusions

A new method to measure the ^{55}Fe content in radioactive samples using GEMPix, a gas detector with pixelated readout, has been developed. A procedure to measure the background and the total counts of a sample has been designed. In total, measurement of one

[14] This is a rough energy calibration such that 6000 TOT counts equal 6000 eV (approximate energy of ^{55}Fe X-rays). In principle this should not be necessary since Eq. (4) already contains a calibration to 5.9 keV. However, it is a way to reduce the impact of the poor fit results from Fig. 19 since only the parameter B is used. The impact of this parameter in the T/P range of interest is sufficiently small to allow for good HV correction (compare Fig. 20).

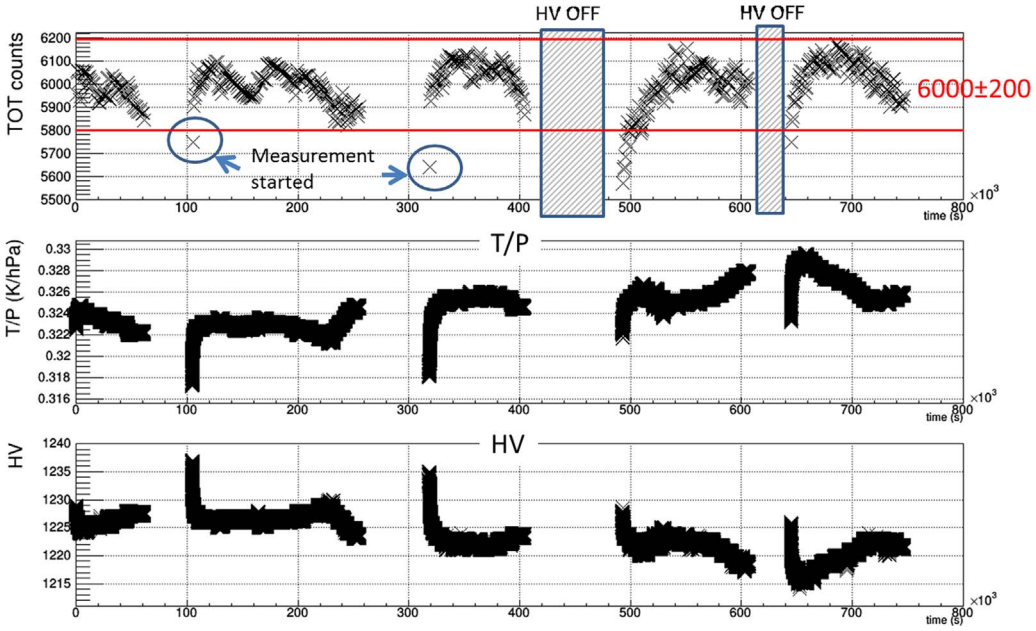

Fig. 20. Measurement with a ^{55}Fe source over nine days. The plots show the time evolution of the TOT counts (top plot), the ratio temperature/pressure (T/P), and the High Voltage (HV). The TOT counts are within 6000 ± 200 if measurements in the heat-up phase of the detector ('fast rising T') and after the HV was off are discarded.

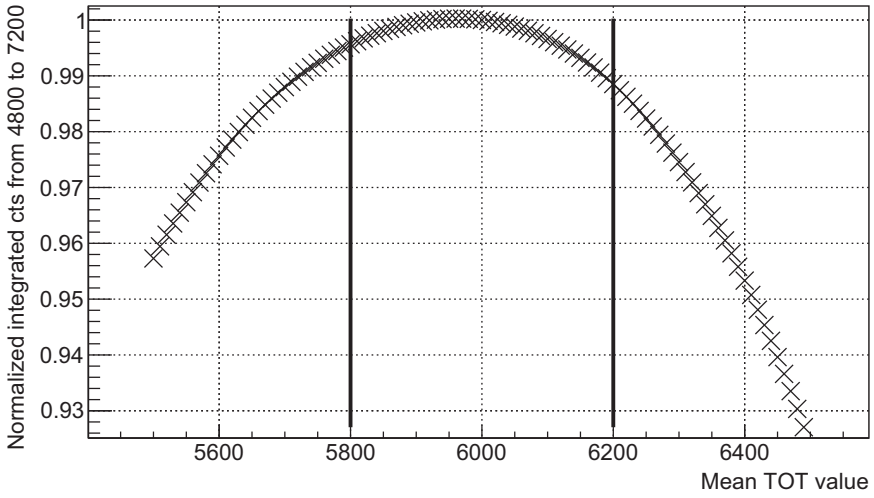

Fig. 21. Conversion of the fluctuation of the mean TOT count value to an uncertainty on the number of event counts. The number of event counts is normalized to the number of event counts at a TOT mean value of 6000. Vertical lines denote maximum deviation of the mean TOT value in the control measurement presented in Fig. 20.

sample takes approximately 4.5 h. Forty-five samples from CERN's radioactive waste were used to calibrate the detector. Measured counts are converted into specific activity using a calibration curve based on reference data from radiochemical analyses of the same samples.

Since the background is sample-dependent, the detection limit is also background-dependent and has been accounted for in the calculation of the detection limits. From the forty-five samples analyzed, good agreement has been found between the radiochemical analysis and the present procedure. As an example, the sensitivity to 30 Bq/g, which is the current Swiss exemption limit for ^{55}Fe, was investigated but only statistical uncertainties of the method were included. The method is potentially sensitive to the exemption limit. A complete uncertainty study is in progress. This will most likely reduce the sensitivity of the method though this will be less important in the future since the activity of most of the samples is small compared to the future Swiss exemption limit of 1 kBq/g.

A correction of the high voltage (and therefore of the gain) as function of temperature, pressure and humidity in the detection volume was developed in order to obtain a more stable system and reduce systematic uncertainties. An operational test phase for this method is planned at CERN.

Acknowledgements

We wish to thank Stuart George (formerly CERN, now with the University of Houston) and Erik Frojd (formerly CERN, now with PSI, Switzerland) for useful discussions. The authors warmly acknowledge Jerome Alozy and Michael Campbell from the Medipix collaboration for the support on the readout electronics. This work was partly supported by the Wolfgang Gentner Programme of the German Ministry of Education and Research and by the Marie Curie Initial Training Network Fellowship of the European Community's Seventh Framework Program under Grant Agreement PITN-GA-4 2011-289198-ARDENT.

References

[1] IAEA, Strategy and Methodology for Radioactive Waste Characterization, IAEA

Nuclear Energy Series, IAEA-TECDOC-1537, 2007.
[2] IAEA, Determination and use of scaling factors for waste characterization in nuclear power plants, IAEA Nuclear Energy Series, NW-T-1.18, 2009.
[3] INternational Organization For Standardization, Nuclear Energy – Nuclear Fuel Technology – Scaling Factor Method to Determine the Radioactivity of Low- and Intermediate-level Radioactive Waste Packages Generated at Nuclear Power Plants, ISO 21238:2007, ISO, Geneva, 2007.
[4] ANDRA, Spécification, Critères radiologiques d'acceptation des déchets TFA, SUR. SP.AMES.02.0007 (CERN EDMS 1332211), ANDRA (2013).
[5] M. Magistris et al., Radionuclide inventory of metallic, TFA radioactive waste, Tech. Note CERN-RP-2015-27-REPORTS-TN EDMS 1501107, 2015.
[6] Ordonnance sur la radioprotection (ORaP), 814.501, Le Conseil Fédéral suisse, 22 juin 1994 (Etat le 1er janvier 2014).
[7] Amec Foster Wheeler's Analytical Services radiochemical laboratory, Private Communication, 2015.
[8] M. Nikl, Scintillation detectors for x-rays, Meas. Sci. Technol. 17 (2006) R37–R54.
[9] F. Murtas, Applications of triple GEM detectors beyond particle and nuclear physics, JINST 9 (2014) C01058.
[10] F. Sauli, GEM: a new concept for electron amplification in gas detectors, Nucl. Instrum. Methods A 386 (1997) 531.
[11] G. Corradi, F. Murtas, D. Tagnani, A novel high-voltage system for a triple GEM detector, Nucl. Instrum. Methods A 572 (2007) 96.
[12] M. Alfonsi, et al., High-rate particle triggering with triple-GEM detector, Nucl. Instrum. Methods A 518 (2004) 106.
[13] V. Kraus et al., FITPix: Fast Interface for Timepix Pixel detectors, 2011, JINST 6 C01079.
[14] D. Turecek et al., Pixelman: a multi-platform data acquisition and processing software package for Medipix2, Timepix and Medipix3 detectors, 2011, JINST 6 C01046.
[15] S.P. George, et al., Particle tracking with a Timepix based triple GEM detector, JINST 10 (2015) P11003.
[16] X. Llopart, et al., Timepix, a 65k programmable pixel readout chip for arrival time, energy and/or photon counting measurements, Nucl. Instrum. Methods A 581 (2007) 485 (Erratum ibid. A 585 (2008), p. 106).
[17] Medipix website: ⟨http://medipix.web.cern.ch/medipix/⟩, (accessed 01.12.16).
[18] M. Campbell, 10 years of the Medipix2 Collaboration, Nucl. Instrum. Methods A 633 (2011) S1.
[19] S.P. George, et al., Measurement of an accelerator based mixed field with a Timepix detector, JINST 10 (2015) P03005.
[20] LHCb collaboration, D. Hynds, The Timepix telescope for charged particle tracking, Nucl. Instrum. Methods A 730 (2013) 50.
[21] ATLAS MPX, MEDIPIX collaborations, E.H.M. Heijne, et al., Measuring radiation environment in LHC or anywhere else, on your computer screen with Medipix, Nucl. Instrum. Methods A 699 (2013) 198.
[22] T. Whyntie, et al., CERN@school: demonstrating physics with the Timepix detector, Contemp. Phys. (2015) 1.
[23] N. Stoffle, et al., Timepix-based radiation environment monitor measurements aboard the International Space Station, Nucl. Instrum. Methods A 782 (2015) 143.
[24] L. Pinsky, et al., Application of the Medipix2 technology to space radiation dosimetry and hadron therapy beam monitoring, Nucl. Instrum. Methods A 628 (2011) 226.
[25] J.H. Hubbell, S.M. Seltzer, Tables of X-ray mass attenuation coefficients and mass energy-absorption coefficients 1 keV to 20 MeV for elements Z=1 to 92 and 48 additional substances of dosimetric interest, NISTIR 5632 (1995).
[26] T. Holy, et al., Pattern recognition of tracks induced by individual quanta of ionizing radiation in Medipix2 silicon detector, Nucl. Instrum. Methods A 591 (2008) 287–290.
[27] Website of AMEC company: ⟨http://www.amecfw.com/⟩, (accessed 01.12.16).
[28] N. Gehrels, Confidence limits for small numbers of events in astrophysical data, Astrophys. J. Part 1 303 (1986) 336–346.
[29] F. Sauli, et al., Construction, test and commissioning of the triple-gem tracking detector for compass, Nucl. Instrum. Methods A 490 (2002) 177–203.